Program Digest, 2019 IEEE International Ultrasonics Symposium (IUS)
Glasgow, Scotland, October 6-9, 2019

Novel FEM Models of Intermodulation Effects in BAW and SAW Devices

Xiangnan Pang, Yook-Kong Yong, Rutgers University, Piscataway, NJ, 08854, USA

***Abstract*—The nonlinear intermodulation effect in piezoelectric devices was studied By using the three-dimensional equations of nonlinear piezoelectricity and the method of harmonic balance, we have formulated and derived coupled sets of nonlinear piezoelectric equations in the frequency domain for intermodulation effects. The coupled sets of equations could be embedded in COMSOL FEM models. In order to check the validity and accuracy of the FEM models we studied the third order intermodulation effects in AT-cut quartz resonators. Our three-dimensional FEM model results compared well with the analytical one-dimensional results by Tiersten and with the experimental results by Smythe. The FEM models could be used for simulating intermodulation effects in BAW and SAW piezoelectric devices provided that the nonlinear material constants are available and are accurate.**

***Index Terms*—Intermodulation distortion effect, nonlinear acoustoelectric behaviors, quartz resonators, bulk acoustic waves (BAW), surface acoustic waves (SAW), finite element method (FEM).**

I. Introduction

We study a class of nonlinear vibrations of BAW and SAW resonators that include amplitude-frequency effects, harmonic generation and intermodulation. Signal distortions, leakage of transmitted signals from an intended band, increase of noise levels, and reduction of sensitivities in wireless mobile application are the results of these types of nonlinear vibrations.

In our previous work [1, 2], the coupled sets of piezoelectric field equations for nonlinear harmonic response were derived. We had embedded the coupled sets of equations in FEM models of COMSOL software, and using the FEM models we had studied amplitude frequency effects in quartz AT-cut resonators and harmonic generation in 128° YX $LiNbO_3$ SAW resonators. The FEM model results for amplitude frequency effects in quartz AT-cut resonators and harmonic generation in 128° YX $LiNbO_3$ SAW resonators respectively compared well with the results by Kubena et. al. [3] and Solal et. al. [4].

In this work we extend our previous work to study intermodulation effects in BAW and SAW resonators. We first derive coupled sets of nonlinear piezoelectric equations for intermodulation distortion effects from the 3-D nonlinear piezoelectric equations, and then embed the coupled sets of equations in 3-D FEM models of COMSOL software. COMSOL Multiphysics software has the features of providing users with the flexibility to modify and extend the built-in modules to implement user-specified coupling

We have studied the IMD3 behavior of the fundamental 11.7 MHz and fifth overtone 111.5 MHz quartz AT-cut resonators. In order to test the validity and accuracy of the FEM models, we have compared our 3-D FEM model results with Tiersten's [5] analytical results and Smythe's [6] measured results. Our FEM model results compared well with both Tiersten's and Smythe's work.

II. Theory and Formulation of Coupled Sets of Nonlinear Piezoelectric Field Equations for Intermodulation Effects.

We could derive the coupled sets of nonlinear piezoelectric field equations for IMD2 and IMD3 in a manner similar to our derivations for harmonic generation in Ref.[1]. We start from the basic nonlinear theory of electro elasticity shown in Eqns. 1-10 below, and in the subsequent sections derive the coupled sets of nonlinear piezoelectric equations for IMD3.

A. Nonlinear Equations of Piezoelectricity

Equations of motion and charge equations of electrostatics:

$$(T_{ij} + T_{jk}U_{i,k})_{,j} = \rho \ddot{U}_i \tag{1}$$

$$D_{i,i} = 0 \tag{2}$$

Piezoelectric constitutive equations including nonlinear terms:

$$T_{ij} = C_{ijkl}S_{kl} + \tfrac{1}{2}C_{ijklmn}S_{kl}S_{mn} + \tfrac{1}{6}C_{ijklmnpq}S_{kl}S_{mn}S_{pq} + \eta_{ijkl}\dot{S}_{kl} - e_{kij}E_k - e_{kijmn}E_kS_{mn} \quad (3)$$

$$D_i = e_{ijk}S_{jk} + \tfrac{1}{2}e_{ijklm}S_{jk}S_{lm} + \varepsilon_{ik}E_k + \tfrac{1}{2}\varepsilon_{ijk}E_jE_k \quad (4)$$

Strain-displacements and electric field-potential relations:

$$S_{ij} = \tfrac{1}{2}(U_{i,j} + U_{j,i} + U_{k,i}U_{k,j}) \quad (5)$$

$$E_i = -\varphi_{,i} \quad (6)$$

Mechanical and electrical boundary conditions:

$$\left(T_{ij} + T_{jk}U_{i,k}\right)n_j = \bar{\bar{T}}_i \quad on\ \Gamma_1 \quad (7)$$

$$U_i = \widehat{U}_i \quad on\ \Gamma_2 \quad (8)$$

$$\varphi_i = \hat{\varphi}_i \quad on\ \Gamma_3 \quad (9)$$

$$n_iD_i = 0 \quad on\ \Gamma_4 \quad (10)$$

The terms U_i, T_{ij}, S_{kl}, φ, E_i, and D_i are the mechanical displacement, stress, strain, electric potential, electric field, electrical displacement fields, respectively. The terms C_{ijkl}, C_{ijklmn}, and $C_{ijklmnpq}$ are the second-, third-, and fourth-order elastic constants; $\eta_{ijkl}$is the viscosity tensor; e_{ijk} and e_{ijklm} are the second-, and third-order piezoelectric constants; ε_{ik} and ε_{ijk} are the second-, and third-order dielectric constants; ρ is the mass density, n_i is the unit normal vector at the boundaries; $\bar{T}_i$, $\bar{U}_i$, and $\bar{\varphi}_i$ are specified stress, mechanical displacement, and electric potential at certain boundaries.

B. Derivation of Coupled Sets of Nonlinear Piezoelectric Field Equations for IMD3

We planned on studying the IMD3 in AT-cut quartz resonators. By the method of harmonic balance [7] only the cubic terms in the constitutive Eqs.(3-4) could cause the IMD3 while the quadratic terms do not contribute to the IMD3. Since the piezoelectric coupling in quartz is weak we could neglect the cubic terms in the electric displacement constitutive Eq.(4).

When two test tones at frequencies f_1 and f_2 are applied to drive a piezoelectric resonator, the frequency response of the resonator will have mechanical and electric fields vibrating at not only frequencies f_1 and f_2(assume $f_1 > f_2$), but also at frequencies $3f_1$, $2f_1 + f_2$, $2f_1 - f_2$, $f_1 + 2f_2$, $2f_2 - f_1$, and $3f_2$. If the frequencies f_1 and f_2 are close to the resonance frequency f_r, then the frequencies $2f_1 - f_2$, $2f_2 - f_1$ are also close to f_r while the frequencies $3f_1$, $2f_1 + f_2$, $f_1 + 2f_2$, and $3f_2$ are close to $3f_r$ the third harmonic overtone of the resonator. Since we are interested specifically in IMD3 in the neighborhood of the main mode resonance frequency f_r, we could neglect the terms associated with the frequencies close to $3f_r$. Therefore, we could write all the field variables as a Fourier sum of four frequency components $f_1, f_2, f_3 = (2f_1 - f_2)$ and $f_4 = (2f_2 - f_1)$. The stress T_{ij}, electric displacement D_i, mechanical displacement U_i and electric potential φ are then Fourier sums of their frequency components $f_n, n = 1, 2, 3, 4$, as follow:

$$T_{ij} = \sum_{n=1}^{4} \frac{1}{2}\left(T_{ij}^{fn}e^{i\Omega_n t} + \bar{T}_{ij}^{fn}e^{-i\Omega_n t}\right) \quad (11)$$

$$D_i = \sum_{n=1}^{3} \frac{1}{2}\left(D_i^{fn}e^{i\Omega_n t} + \bar{D}_i^{fn}e^{-i\Omega_n t}\right) \quad (12)$$

$$U_i = \sum_{n=1}^{4} \frac{1}{2}\left(U_i^{fn}e^{i\Omega_n t} + \bar{U}_i^{fn}e^{-i\Omega_n t}\right) \quad (13)$$

$$\varphi = \sum_{n=1}^{4} \frac{1}{2}\left(\varphi^{fn}e^{i\Omega_n t} + \bar{\varphi}^{fn}e^{-i\Omega_n t}\right) \quad (14)$$

where $\Omega_n = 2\pi f_n$, and T_{ij}^{fn}, D_i^{fn}, U_i^{fn}, and φ^{fn} are the frequency components of stress, electric displacements, mechanical displacements and electric potential respectively. The terms with an overhead bar are their respective complex conjugate counterparts.

Upon substitution of Eqs.(13 and 14) into Eqs.(5 and 6) respectively we obtain the Fourier sums of their frequency components for the strain-displacement relations and electric field-potential relations:

$$S_{ij} = \sum_{n=1}^{3} \frac{1}{2}\left(S_{ij}^{fn}e^{i\Omega_n t} + \bar{S}_{ij}^{nf}e^{-i\Omega_n t}\right) \quad (15)$$

$$E_i = \sum_{n=1}^{3} \frac{1}{2}\left(E_i^{fn}e^{i\Omega_n t} + \bar{E}_i^{fn}e^{-i\Omega_n t}\right) \quad (16)$$

where $S_{ij}^{fn} = \tfrac{1}{2}(U_{i,j}^{fn} + U_{j,i}^{fn} + U_{k,i}^{fn}U_{k,j}^{fn}) \quad (17)$

and $E_i^{fn} = -\varphi_{,i}^{fn} \quad (18)$

The Fourier sums of frequency components for the strain-displacement relations and electric field potential relations in Eqs.(15-16) are then substituted into the piezoelectric constitutive equations of Eqs.(3-4), and by employing the method of harmonic balance [7] we could obtain the constitutive equations for each frequency component of stress and electric displacements T_{ij}^{fn}, and D_i^{fn} $(n = 1, 2, 3, 4)$, respectively, in terms of the frequency components of strain and electric field S_{ij}^{fn}, and ${E_i}^{fn}$ as follow:

$$T_{ij}^{f_1} = C_{ijkl}S_{kl}^{f_1} + \eta_{ijkl}\dot{S}_{kl}^{f_1} - e_{kij}E_k^{f_1} + \frac{1}{3}C_{ijklmnpq}\Big(\frac{3}{8}S_{kl}^{f_1}S_{mn}^{f_1}\bar{S}_{pq}^{f_1} + \frac{3}{8}S_{kl}^{f_2}S_{mn}^{f_2}\bar{S}_{pq}^{f_4} + \frac{3}{4}S_{kl}^{f_1}S_{mn}^{f_2}\bar{S}_{pq}^{f_2} + \frac{3}{4}S_{kl}^{f_1}S_{mn}^{f_3}\bar{S}_{pq}^{f_3} + \frac{3}{4}S_{kl}^{f_1}S_{mn}^{f_4}\bar{S}_{pq}^{f_4} + \frac{3}{4}S_{kl}^{f_2}S_{mn}^{f_3}\bar{S}_{pq}^{f_1} + \frac{3}{4}S_{kl}^{f_3}S_{mn}^{f_4}\bar{S}_{pq}^{f_2}\Big) \quad (19)$$

$$T_{ij}^{f_2} = C_{ijkl}S_{kl}^{f_2} + \eta_{ijkl}\dot{S}_{kl}^{f_2} - e_{kij}E_k^{f_2} + \frac{1}{3}C_{ijklmnpq}\Big(\frac{3}{8}S_{kl}^{f_2}S_{mn}^{f_2}\bar{S}_{pq}^{f_2} + \frac{3}{8}S_{kl}^{f_1}S_{mn}^{f_1}\bar{S}_{pq}^{f_3} + \frac{3}{4}S_{kl}^{f1}S_{mn}^{f2}\bar{S}_{pq}^{f1} + \frac{3}{4}S_{kl}^{f_2}S_{mn}^{f_3}\bar{S}_{pq}^{f_3} + \frac{3}{4}S_{kl}^{f_2}S_{mn}^{f_4}\bar{S}_{pq}^{f_4} + \frac{3}{4}S_{kl}^{f_1}S_{mn}^{f_4}\bar{S}_{pq}^{f_2} + \frac{3}{4}S_{kl}^{f_3}S_{mn}^{f_4}\bar{S}_{pq}^{f_1}\Big) \quad (20)$$

$$T_{ij}^{f_3} = C_{ijkl}S_{kl}^{f_3} + \eta_{ijkl}\dot{S}_{kl}^{f_3} - e_{kij}E_k^{f_3} + \frac{1}{3}C_{ijklmnpq}\Big(\frac{3}{8}S_{kl}^{f_1}S_{mn}^{f_1}\bar{S}_{pq}^{f_2} + \frac{3}{8}S_{kl}^{f_3}S_{mn}^{f_3}\bar{S}_{pq}^{f_3} + \frac{3}{4}S_{kl}^{f_2}S_{mn}^{f_3}\bar{S}_{pq}^{f_2} + \frac{3}{4}S_{kl}^{f_3}S_{mn}^{f_4}\bar{S}_{pq}^{f_4} + \frac{3}{4}S_{kl}^{f_1}S_{mn}^{f_3}\bar{S}_{pq}^{f_1} + \frac{3}{4}S_{kl}^{f_1}S_{mn}^{f_2}\bar{S}_{pq}^{f_4}\Big) \quad (21)$$

$$T_{ij}^{f_4} = C_{ijkl}S_{kl}^{f_4} + \eta_{ijkl}\dot{S}_{kl}^{f_4} - e_{kij}E_k^{f_4} + \frac{1}{3}C_{ijklmnpq}\Big(\frac{3}{8}S_{kl}^{f_2}S_{mn}^{f_2}\bar{S}_{pq}^{f_1} + \frac{3}{8}S_{kl}^{f_4}S_{mn}^{f_4}\bar{S}_{pq}^{f_4} + \frac{3}{4}S_{kl}^{f_1}S_{mn}^{f_4}\bar{S}_{pq}^{f_1} + \frac{3}{4}S_{kl}^{f_4}S_{mn}^{f_3}\bar{S}_{pq}^{f_{12}} + \frac{3}{4}S_{kl}^{f_2}S_{mn}^{f_4}\bar{S}_{pq}^{f_2} + \frac{3}{4}S_{kl}^{f_1}S_{mn}^{f_2}\bar{S}_{pq}^{f_3}\Big) \quad (22)$$

$$D_i^{f_1} = e_{ijk}S_{jk}^{f_1} + \varepsilon_{ik}E_k^{f_1} \quad (23)$$

$$D_i^{f_2} = e_{ijk}S_{jk}^{f_2} + \varepsilon_{ik}E_k^{f_2} \quad (24)$$

$$D_i^{f_3} = e_{ijk}S_{jk}^{f_3} + \varepsilon_{ik}E_k^{f_3} \quad (25)$$

$$D_i^{f_4} = e_{ijk}S_{jk}^{f_4} + \varepsilon_{ik}E_k^{f_4} \quad (26)$$

Note that in each of the Eqs.(19-26) there is harmonic balance [7] whereby the frequency of the term on left hand side of each equation is the same as the frequency of each term on the right hand side.

The constitutive equations (Eqs.(19-26)) must respectively satisfy the equations of motion Eq.(1) and charge equations of electrostatics Eq.(2) at each harmonic frequency $f_n, n = 1, 2, 3, 4$. We substitute Eqs.(11-13) into Eqs.(1-2), and by employing the method of harmonic balance [7] we obtain the equations of motion and charge equations of electrostatics at each harmonic frequency $f_n, n = 1, 2, 3, 4$:

$$(T_{ij}^{f_n} + T_{ij}^{f_n}U_{i,\mathrm{k}}^{f_n})_{,j} = \rho\ddot{U}_i^{f_n} \quad (27)$$

$$D_{i,i}^{f_n} = 0 \quad (28)$$

The boundary conditions for Eqs.(27-28) are derived by substitution of Eqs.(11-14) into boundary conditions Eqs.(7-10) to obtain the respective mechanical and electrical boundary conditions at each harmonic frequency $f_n, n = 1, 2, 3, 4$.

$$(T_{ij}^{f_n} + T_{ij}^{f_n}U_{i,\mathrm{k}}^{f_n})n_j = \hat{T}_i^{f_n} \quad on\ \Gamma_1 \quad (29)$$

$$U_i^{f_n} = \hat{U}_i^{f_n} \quad on\ \Gamma_2 \quad (30)$$

$$\varphi^{f_n} = \hat{\varphi}^{f_n} \quad on\ \Gamma_3 \quad (31)$$

$$n_i D_i^{f_n} = 0 \quad on\ \Gamma_4 \quad (32)$$

Eqs.(19-26) are the four sets of constitutive equations for the four sets of governing equations in Eqs.(27-28) that satisfy the four sets of boundary conditions in Eqs.(29-32). Therefore we have four sets of coupled equations for modeling IMD3 in piezoelectric resonators. These four sets of equations are embedded in COMSOL finite elements models.

III. IMD3 OF BAW QUARTZ RESONATORS

We study first the IMD3 in BAW quartz resonators because our literature review found that it was well studied both analytically and experimentally. Tiersten [5] derived the relationship between the nonlinear material constants of AT-cut quartz necessary for the IMD3 analysis and the IMD3 electric current of AT-cut quartz resonators. Smythe [6] had measured the IMD3 of two groups of AT-cut quartz resonators, and employed the analytical results by Tiersten to calculate a nonlinear material parameter that included the fourth order elastic constant C_{6666}.

The dimensions for an AT-cut quartz resonator studied by Tiersten and Smythe [5, 6] is shown in Fig.1a. A schematic diagram of the test circuit of the resonator is shown in Fig.1b. Since the piezoelectric coupling in quartz is very weak, and the vibration mode in the AT-cut quartz resonator is thickness shear vibration along the thickness direction, Tiersten had developed an essentially one-dimensional model of the trapped energy AT-cut quartz resonator. The IMD3 in quartz resonators is due to the cubic term in Eq.(3) which involved the fourth order elastic tensor. Tiersten showed for the AT-cut quartz resonators the fourth order elastic constant C_{6666} and some third order elastic constants together formed a parameter that could be measured in IMD3 experiments.

Smythe [6] tested the two groups of AT-cut quartz resonators. The group of resonators with fundamental 11.7 MHz had dimensions: $2h = 0.1395\,mm$, $2h' = 3.25 \times 10^{-4}\,mm$, $2l = 2.54\,mm$, and $2w = 3.81\,mm$, while the group of resonators with 5th overtone 111.455 MHz had dimensions: $2h = 0.07322\,mm$, $2h' = 3.25 \times 10^{-4}\,mm$, $2l = 0.9144\,mm$, and $2w = 1.2954\,mm$. The resonators under test were connected in series with a load resistance and a generator with internal resistance as shown in Fig.1b.

In order to validate and check the accuracy of our coupled sets of nonlinear piezoelectric equations for the IMD3, we compared the results of our three-dimensional COMSOL FEM models of IMD3 with both Tiersten's [5] one-dimensional analysis and Smythe's [6] measured data. Our model FEM results (solid red and green curves) of IMD3 of the two groups of resonators are shown in Fig. (2), along with Tiersten's analytical results (dashed blue and black curves) and Smythe's measured results (blue and black markers). In these results, the term P_{TT} represents the power available from each test tone generator, and the IMD3 is defined as the ratio of test tone power P_{TT} to the intermodulation power P_{IMD3}, that is, $\mathrm{IMD3} = P_{TT}/P_{IMD3}$. For the group of sixteen fundamental 11.7 MHz resonators, Smythe only measured the drive level at the $P_{TT} = 20\ \mathrm{dBm}$, and he obtained $\mathrm{IMD3} = 54.7 \pm 2\ \mathrm{dB}$. For our model FEM results and Tiersten's analytical results we can sweep the test tone power approximately from -60 to 30 dBm. Our model FEM results (solid red line) compared very well with both Tiersten's analytical results (dashed blue line) and Smythe's measured result (blue delta marker).

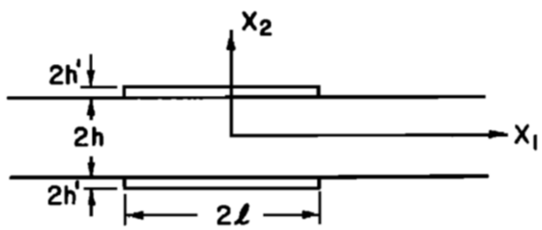

(a)

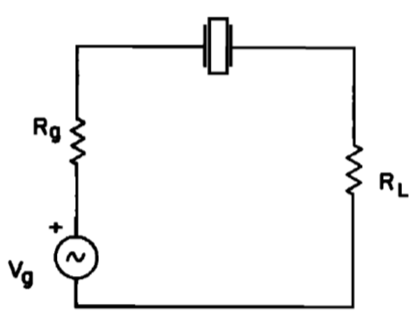

(b)

Fig.1.(a) A schematic diagram of the 11.67 MHz AT-cut quartz resonator with dimensions $2h = 0.1395\ mm$, $2h' = 3.25 \times 10^{-4}\ mm$, $2l = 2.54\ mm$, $2w = 3.81\ mm$, where $2w$ is dimension in X_3 direction and not shown in the figure, (b) A schematic diagram of test circuit of the resonator [6]. The symbols V_g, R_g, and R_L represent the generator voltage, generator resistance and load resistance, respectively.

For the group of fourteen 111.5 MHz fifth overtone resonators, Smythe's measurements were performed with test tone power $P_{TT} = 0\ \mathrm{dBm}$. Our model FEM results (solid green line) compared very well with both Tiersten's analytical results (dashed black line) and Smythe's measured result (black round marker). The results comparisons in Fig. 2 validated our coupled sets of nonlinear piezoelectric equations for the IMD3 and the accuracy of our three-dimensional FEM models.

IV. CONCLUSION

Coupled sets of nonlinear piezoelectric field equations for the third order intermodulations were derived consistently from the three-dimensional nonlinear piezoelectric equations. The method of harmonic balance was employed to derive the equations in the frequency domain. The accuracy of formulation was validated using COMSOL FEM models for the third order intermodulation effects in AT-cut quartz resonators. Our FEM model IMD3 results compared well with the analytical IMD3 results by Tiersten [5], and with the experimental results by Smythe [6]. Our formulation and derivation of the coupled sets of equations for intermodulation are general and are applicable for any piezoelectric resonator.

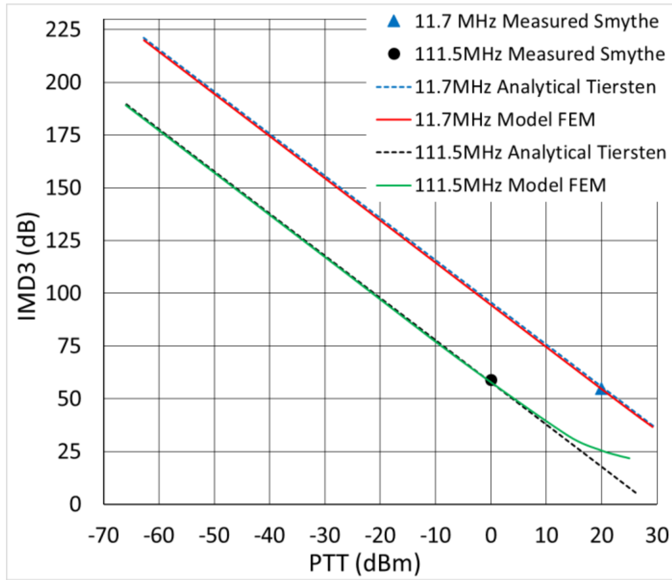

Fig.2. The third order intermodulation distortion effect (IMD3) of two groups of AT-cut quartz resonators.

References

[1] Y. K. Yong, X. Pang, and J. Wang. "Special Nonlinear Effects of the Harmonic 3rd Overtone Thickness-Shear Mode on its Fundamental Mode in F-3F Modal Interactions and Drive Level Dependency." *2018 IEEE International Ultrasonics Symposium (IUS)*. IEEE, 2018.

[2] X. Pang and Y-K Yong, "Characteristics of BAW Modes Harmonically Generated (f-2f-3f) in $LiNbO_3$ SAW Devices.", Proceedings of the 2019 IFCS. ISBN number 978-1-5386-8305-7/19.

[3] "Special Amplitude-Frequency Effects in VHF Quartz Resonators", Randall Kubena, Richard Joyce, Brian Rose and Yook-Kong Yong, Proceedings of the 2014 IEEE International Frequency Control Symposium, Taipei, Taiwan, 2014, pp. 1-6, DOI: 10.1109/FCS.2014.6859982.

[4] M. Solal, K. Kokkonen, S. Inoue, J. Briot, B. Abbott, and K. Gamble, "Observation for nonlinear harmonic generation of bulk modes in SAW devices," *IEEE Trans. Ultrason., Ferroelect., Freq. Control*, vol. 64, no. 9, pp. 1361–1367, Sep. 2017.

[5] H. F. Tiersten, "Analysis of intermodulation in thickness-shear and trapped energy resonators," *J. Acoust. Soc. Am.*, vol. 57, no. 3, pp. 667-681, Mar. 1975.

[6] R. C. Smythe, "Intermodulation in thickness-shear resonators," in *Proc. 28th Annu. Symp. Freq. Control.*, 1974, pp. 5–7.

[7] Marinca V., Herisanu N. (2012) The Method of Harmonic Balance. In: Nonlinear Dynamical Systems in Engineering. Springer, Berlin, Heidelberg, **DOI** https://doi.org/10.1007/978-3-642-22735-6_3